Available online at www.sciencedirect.com
SCIENCE DIRECT
ELSEVIER
Earth and Planetary Science Letters 236 (2005) 322–338
EPSL
www.elsevier.com/locate/epsl

A 25 m.y. isotopic record of paleodiet and environmental change from fossil mammals and paleosols from the NE margin of the Tibetan Plateau

Yang Wang [a,*], Tao Deng [b]

[a] *Department of Geological Sciences, Florida State University and National High Magnetic Field Laboratory, Tallahassee, FL 32306-4100, USA*
[b] *Institute of Vertebrate Paleontology and Paleoanthropology, Chinese Academy of Sciences, Beijing, P.R. China*

Received 24 August 2004; received in revised form 27 April 2005; accepted 9 May 2005
Available online 20 June 2005
Editor: E. Boyle

Abstract

We use the carbon and oxygen isotopic compositions of fossil tooth enamel and paleosols to reconstruct the late Cenozoic history of vegetation and environmental change in the Linxia Basin at the northeastern margin of the Tibetan Plateau. The $\delta^{13}C$ values of fossil enamel from a diverse group of herbivores and of paleosol carbonate and organic matter indicate that C4 grasses were either absent or insignificant in the Linxia Basin prior to ~2–3 Ma and only became a significant component of local ecosystems in the Quaternary. This is in striking contrast to what was observed in Pakistan, Nepal, Africa and the Americas where C4 plants expanded rapidly in the late Miocene as indicated by a positive $\delta^{13}C$ shift in mammalian tooth enamel and paleosols. The $\delta^{18}O$ results from the same herbivore species show several significant shifts in climate in the late Cenozoic. Most notably, a positive $\delta^{18}O$ shift after ~7 Ma indicates a shift to warmer and/or drier conditions and is comparable in timing and direction to the $\delta^{18}O$ shift observed in paleosol carbonates in Pakistan and Nepal. This late Miocene climate change observed in the Indian sub-continent and in the Linxia Basin, however, seems to be a regional manifestation of a global climate change. The lack of evidence for C4 plants in the Linxia Basin prior to ~2–3 Ma suggests that the East Asian summer monsoon, which brings precipitation into northern China during the summer and creates optimal conditions for the growth of C4 grasses, was probably not strong enough to affect this part of China throughout much of the Neogene. This implies that the Himalayan-Tibetan Plateau may not have reached the present-day elevation across its vast extent to support a strong East Asian monsoon system before ~2–3 Ma. Our data also suggest that regional climatic conditions played an important role in controlling the expansion of C4 plants.

Keywords: carbon isotopes; oxygen isotopes; tooth enamel; Tibetan Plateau; paleodiet; paleoecology; climate change

* Corresponding author. Tel.: +1 850 644 1121; fax: +1 850 644 0827.
E-mail address: ywang@magnet.fsu.edu (Y. Wang).

0012-821X/$ - see front matter © 2005 Elsevier B.V. All rights reserved.
doi:10.1016/j.epsl.2005.05.006

1. Introduction

Stable carbon and oxygen isotopes in mammalian tooth enamel and in soil carbonate and organic matter preserve a proxy record of paleoecology and paleoclimate in terrestrial ecosystems [1–4]. Specifically, the carbon isotopes in tooth enamel or in soil carbonate and organic matter record the photosynthetic pathways associated with C3, C4 and CAM plants that are ingested by mammalian herbivores or are growing in the soil, respectively [e.g.,1–4]. The oxygen isotopes in tooth enamel reflect the isotopic composition of local meteoric water, which in turn is related to climate (e.g., [1–4]). C3 plants use the C3 photosynthetic pathway and include trees, shrubs, forbs and cool climate grasses. C4 plants use the C4 photosynthetic pathway and have CO_2-concentrating mechanisms that offer a competitive advantage over C3 plants at low pCO_2 (i.e.,<500 ppm) levels [4]. The photosynthetic efficiency of C3 grasses relative to C4 grasses varies with both pCO_2 and temperature such that C4 grasses are favored under low pCO_2 conditions when accompanied by high temperature [4]. In the modern world, C4 plants are mostly warm climate grasses and dominate in warm regions with summer precipitation, and the transition from C4 to C3 grasses takes places between 30° and 45° latitude with C3 grasses being dominant in cooler regions at high latitudes and altitudes [4]. CAM plants (using crassulacean acid metabolism) include many of the succulent plants and are common in deserts but are rare in other ecosystems.

Isotopic evidence from mammalian tooth enamel and paleosols from around the world indicates a major change in the terrestrial environment during the late Miocene (e.g., [4–6]). Prior to the late Miocene, terrestrial ecosystems in low-to mid-latitude and low-elevation regions were fundamentally different than they are today. They consisted primarily of C3 plants. C4 grasses, which are common in low-elevation (below 3000 m) tropical, subtropical and temperate ecosystems today [7,8], either did not exist or were a minor component of the local biomass until ~7–5 Ma as indicated by a positive $\delta^{13}C$ shift in mammalian tooth enamel and paleosols in many places around the world [4–6,9–17]. It has been hypothesized that the late Miocene expansion of C4 plants around the world

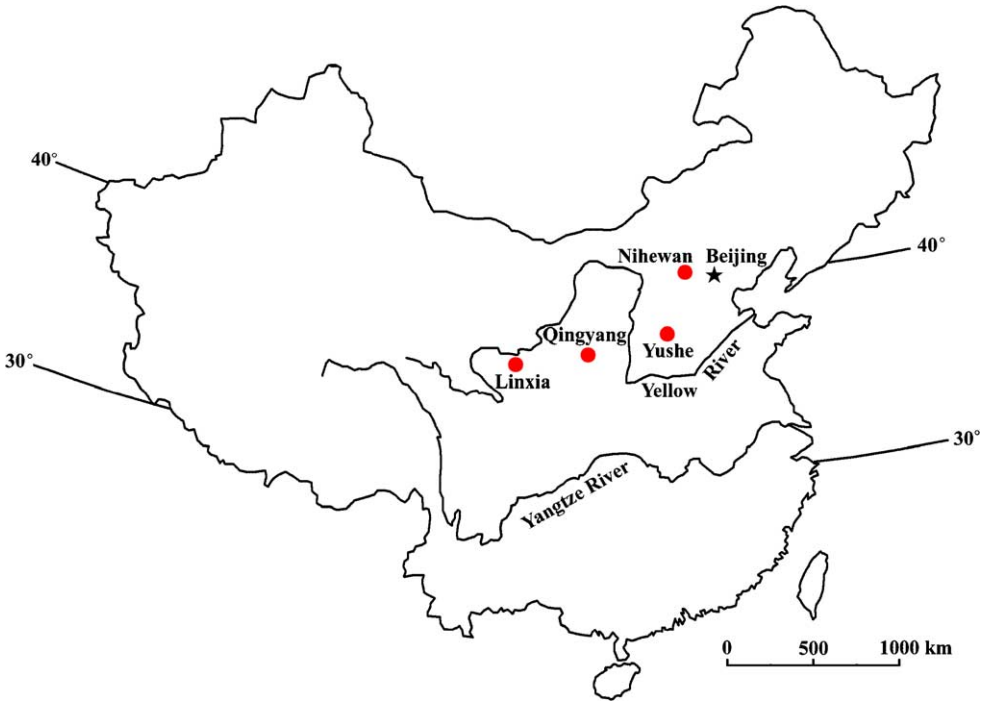

Fig. 1. A map showing the Linxia Basin and other study sites in northern China.

occurred in response to either declining atmospheric carbon dioxide levels [4–6,10] and/or strengthening of the Asian summer monsoon system caused by the rapid uplift of the Himalayan-Tibetan Plateau in the late Miocene [12,13]. However, other studies suggest that there was no global expansion of C4 plants in the

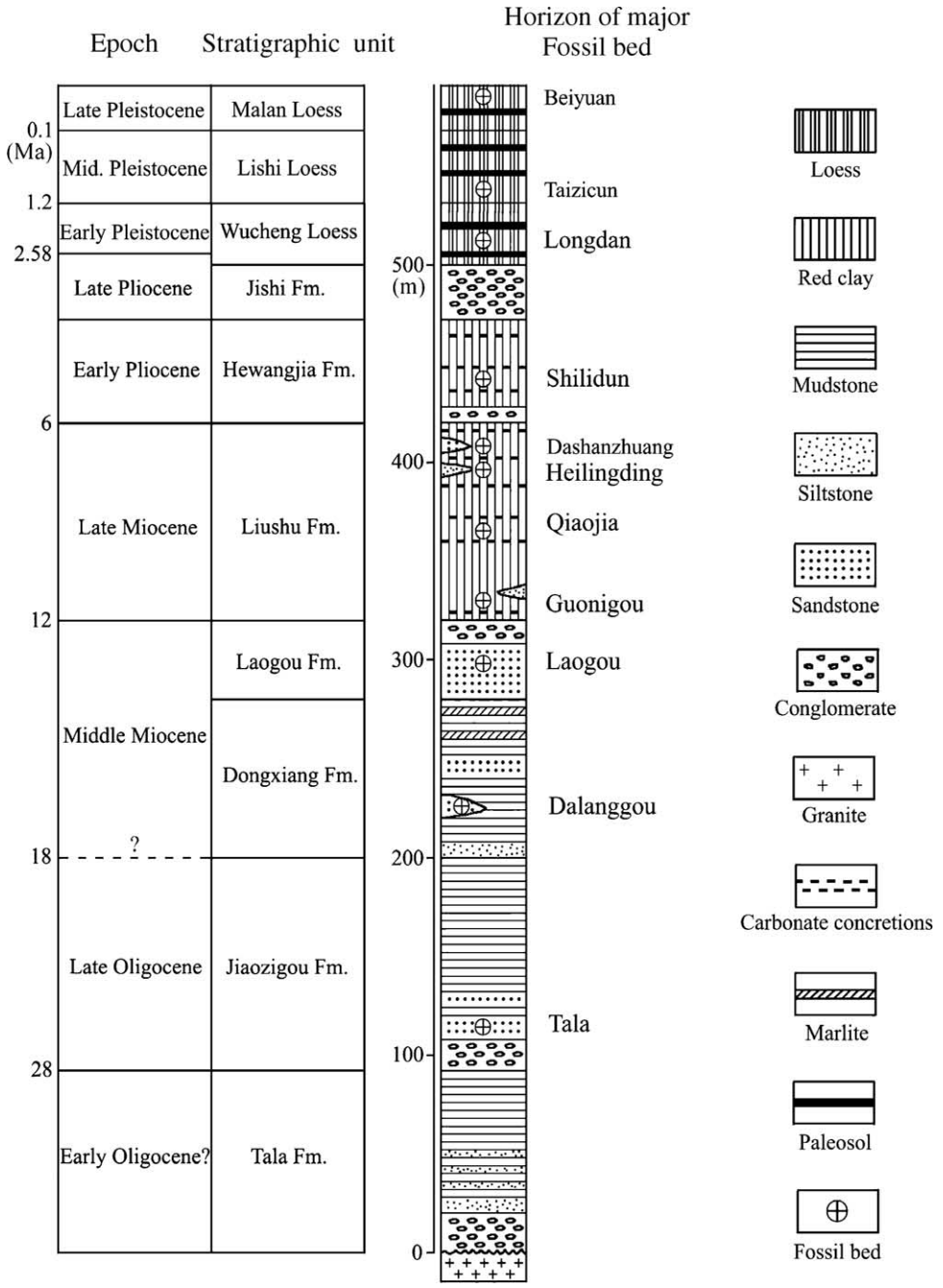

Fig. 2. Sedimentary sequence in the Linxia Basin (after Fang et al. [27,28]; Deng et al. [29]).

late Miocene [18–20] and there is no evidence for major changes in atmospheric CO_2 levels during the Miocene [21–23]. Paleovegetation records in China are sparse, particularly for the critical period of "global" C4 expansion (i.e., late Miocene).

Here we present the results of stable isotopic analyses of mammalian herbivores and soils from a late Cenozoic sequence in the Linxia Basin in northern China, spanning an age range from ~25 Ma to the present. Our isotope data are interpreted in terms of changes in paleodiet, paleovegetation and paleoclimate. The goal of our study is to determine if the major global changes in vegetation and climate seen elsewhere also occurred in northern China. Comparison of our data from northern China with those from other parts of the world allows for a better understanding of the causes and patterns of the development of C4 ecosystems in the late Neogene and can shed light on the timing history of the uplift of the Himalayan-Tibetan Plateau.

2. Geographic and geological setting

The Linxia Basin (103°E, 35°N) is located just northeast of the topographic front on the northeastern margin of the Tibetan Plateau (Fig. 1). The present-day elevation of the basin is about 1917 m. The present-day ecosystems in the area are classified as "temperate steppe" and have floristic components that include Compositae, Gramineae, Chenopodiaceae, Cyperaceae and Artemisia [24,25]. The Linxia Basin has well-exposed Late Cenozoic sedimentary sequences [26–29] that span late Oligocene to Holocene ages (Fig. 2). The chronology of the sedimentary deposits in the basin has recently been established using a variety of dating techniques, including magnetostratigraphy and biostratigraphy [27–29].

The Linxia Basin is bounded by major faults on the north, west and south, but its lateral extent is not well defined towards the east [28]. Various lines of evidence suggest that the Linxia Basin began to form at about 29 Ma, as a result of the collision of India with Asia that started ~50–70 Ma [27,28,30]. It has been suggested that the northeast margin of the Tibetan Plateau grew in a stepwise fashion towards the northeast through time [28,31] and the deformation front of the Tibetan Plateau had propagated into the Linxia Basin by 6 Ma [28]. The deposits in the basin are primarily composed of fluvial and lacustrine sediments with Pleistocene eolian loess deposits covering much of the area. The stratigraphy in the basin has been divided into ten formations based on lithofacies and paleontology (Fig. 2). The Linxia Basin contains a long sedimentary record with abundant and well-preserved mammalian fossils. The richness and diversity of the fossils in the basin are among the best Neogene terrestrial fossil records in the world. Therefore, the Linxia Basin is an ideal place to study paleovegetation and paleoclimate using stable carbon and oxygen isotopes in mammalian tooth enamel.

3. Sampling and analytical methods

Stable carbon and oxygen isotopes in mammalian tooth enamel are resistant to diagenesis [e.g.,9,32] and are therefore very useful in paleoenvironmental reconstruction. We selected 126 well-preserved fossil teeth for carbon and oxygen isotopic analyses from a diverse group of mammalian herbivores including *Gomphotherium, Platybelodon, Hipparion, Equus, Allacerops, Indricotherium, Alicornops, Chilotherium, Parelasmotherium, Cervavitus, Palaeotragus, Gazella*, and *Leptobos*. The ages of the samples (Fig. 2) were estimated based on the paleomagnetic time scale and stratigraphic positions [27–29]. In addition to fossil teeth, we collected pedogenic carbonates and soil organic matter from both modern soils and buried paleosols (formed in Pleistocene loess deposits) at various localities for carbon isotopic analyses. All the paleosols and modern soils sampled for isotopic analyses have typical soil horizonation with a dark organic rich A horizon and a reddish, leached B horizon that have been thoroughly bioturbated. Pedogenic carbonates in these soils are nodular, typically 1–3 cm in diameter, and are found in a zone located below the B horizon. Pedogenic carbonate nodules were collected from a depth of 40–50 cm below the soil surface. Soil samples for isotopic analysis of organic matter were collected from the A horizon of the soil. Most of the paleosols that we sampled were formed in the late Pleistocene Malan Loess (Fig. 2) and were assigned an age of late Pleistocene. Two pebbles with pedogenic coatings were collected from

paleosols formed in the middle Pleistocene Lishi Loess and were given an estimated age of mid-Pleistocene. Paleosols in the older sections lack organic-rich A horizon but are all rich in carbonate as massive carbonate cementation. Carbonates in these older paleosols were not analyzed because of their uncertain origin.

The tooth enamel of our fossil samples is in an excellent condition and shows little or no sign of alteration. For each sample, we first cut a piece of tooth along the growth axis, manually separated the enamel from dentine and other matrix with a Dremel tool, and then ground it into fine powder using a mortar and pestle. The enamel sample prepared in this way yields an average isotopic signal for the growth period of the tooth. The sample powder was then soaked in 5% sodium hypochlorite (NaOCl) overnight to remove any possible organic contaminants, cleaned with distilled water and freeze-dried. The powder was then treated with 1 M acetic acid under weak vacuum overnight to remove carbonate, cleaned with distilled water and freeze-dried. The resulting powder (containing only hydroxyapatite crystals) was reacted with 100% H_3PO_4 under vacuum over two nights to produce CO_2 from the structural CO_3^{2-} in the apatite [e.g.,10,32]. The CO_2 was then purified cryogenically and its carbon and oxygen isotopic ratios were measured on a Finnigan stable isotope ratio mass spectrometer at the Florida State University. All soil carbonate samples (total 26) and some of the tooth enamel samples were analyzed on a VG Prism in the Stable Isotope Lab at the University of Florida. Prior to analysis, the soil carbonate samples were ground into powder and baked under vacuum at 425 °C for 1 h to carbonize any organic matter in the sample [1,33]. Soil samples for organic matter isotopic measurements were ground into powder, treated with 10% HCl to remove carbonate, rinsed with distilled water, and dried. CO_2 was produced by combustion of the sample with CuO and silver foil in an evacuated quartz tube at 875 °C, purified cryogenically and analyzed on a stable isotope ratio mass spectrometer [1,33]. The carbon and oxygen isotopic ratios of the samples are reported in the standard notation as $\delta^{13}C$ and $\delta^{18}O$ ($\delta = [R_{sample}/R_{standard} - 1] \times 1000$, where $R = {}^{13}C/{}^{12}C$ or ${}^{18}O/{}^{16}O$) relative to the international carbonate standard PDB (Pee Dee Belemnite). The analytical precision (based on replicate analyses of carbonate standard NBS-19 and our lab standard PDA-$CaCO_3$ processed with each batch of samples) for both $\delta^{13}C$ and $\delta^{18}O(CO_3^{2-})$ is better than 0.1‰.

4. Results and discussions

4.1. Carbon isotopes, paleodiet and paleoecology

Structural carbonate in tooth enamel hydroxyapatite is enriched in ^{13}C by about 14‰ relative to diet [6,10,32,34,35]. Therefore, changes in the $\delta^{13}C$ values of tooth enamel bioapatite reflect changes in the diet that were ultimately driven by changes in the isotopic composition of the vegetation. Most plants photosynthesize by either the C3 pathway (C3 plants) or the C4 pathway (C4 plants). C3 plants (i.e., trees, most shrubs and cool climate grasses) have $\delta^{13}C$ values ranging from −22‰ to −34‰ with an average of −27‰ [36–38]. Under water-stressed conditions, C3 plants are enriched in ^{13}C and have $\delta^{13}C$ values higher than the average value of −27‰. Under closed canopies, C3 plants have lower $\delta^{13}C$ values (that can be as low as −34‰) due to the influence of soil respiration [39–41]. C4 plants (mostly warm climate grasses) have $\delta^{13}C$ values of −9 ‰ to −17‰, averaging −13‰. Therefore, for enamel structural carbonate, a $\delta^{13}C$ value of −8‰ or less would indicate a dietary intake of pure C3 plants; whereas a $\delta^{13}C$ value of >−3‰ would indicate a pure C4 diet. Cerling et al. [6] argue that for fossil bioapatite the "cut-off" for a pure C3 diet may be even −7‰ because the burning of fossil fuels has lowered the $\delta^{13}C$ of the atmosphere and plants by 1.5‰ since the beginning of the industrial revolution. For pedogenic carbonate formed at deeper depths (>30 cm) in a soil with moderate to high respiration rates, its carbon isotopic composition is enriched by 14–17‰ relative to co-existing organic matter due to isotope fractionation resulting from equilibrium between $CaCO_3$ and CO_2 and gaseous diffusion in the system [1,42]. As such, a $\delta^{13}C$ value of ~+2‰ for pedogenic carbonate would indicate the presence of a pure C4 biomass whereas a $\delta^{13}C$ value of −12‰ is indicative of a pure C3 flora [1,42].

The carbon isotopic record from analyses of fossil tooth enamel (Fig. 3 and Table 1) and soils (Table 2)

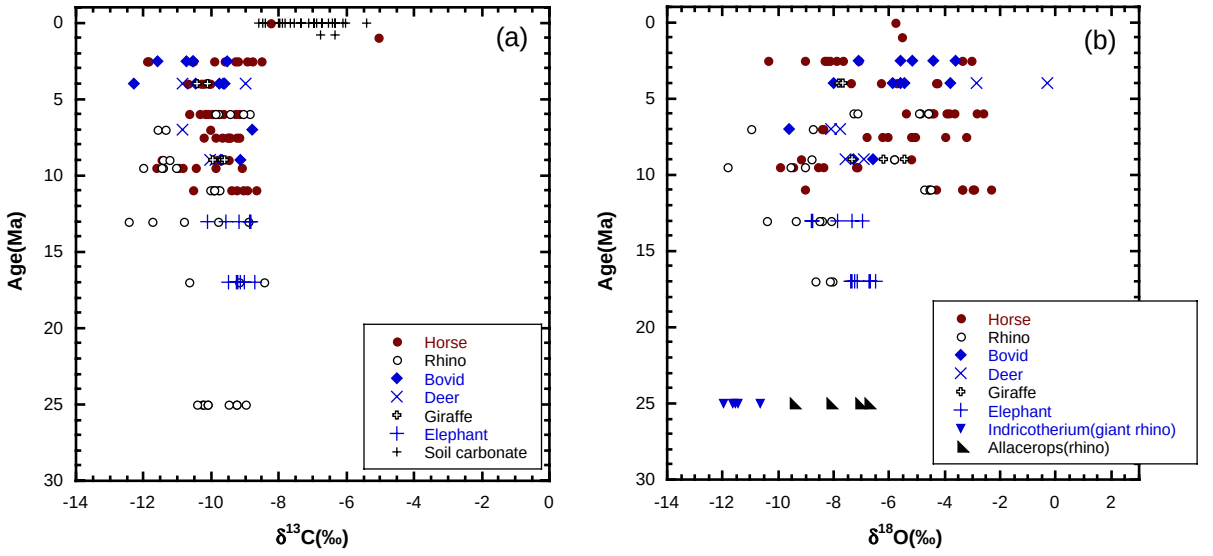

Fig. 3. Stable carbon (a) and oxygen (b) isotopic compositions of tooth enamel of herbivores from the Linxia Basin in northern China. $\delta^{13}C$ values of Holocene and Pleistocene soil carbonates are also plotted in (a) for comparison.

from the Linxia Basin can be divided into two distinct periods:

(1) 25 to ~2.5 Ma: The $\delta^{13}C$ values of tooth enamel from this time interval display a narrow range of variation from −8.4‰ to −12.4‰ (Fig. 3a), with a mean $\delta^{13}C$ value of -10.0 ± 0.9‰ (all means reported ± 1 standard deviation). These $\delta^{13}C$ values indicate that these various herbivores were feeding predominantly on C3 plants during the late Paleogene and Neogene. The highest $\delta^{13}C$ value of −8.4‰ is found in the enamel of a 17 million-year-old rhino (*Alicornops*), which indicates either a small amount of C4 plants in its diet or that the animal was feeding on C3 plants experiencing water stress [43].

The pure or nearly pure C3 diet of various herbivores suggests that the ecosystems in the Linxia Basin consisted primarily of C3 plants prior to ~2–3 Ma (Fig. 3). The $\delta^{13}C$ range of 4‰ in herbivore tooth enamel probably reflects carbon isotopic variations of plants being consumed. The $\delta^{13}C$ values of herbivore tooth enamel from the Linxia Basin for this time interval correspond to a dietary intake of −22.4‰ to −26.4‰, with a mean value of -24.0 ± 0.9‰, which falls well within the $\delta^{13}C$ range of modern C3 plants. However, the inferred $\delta^{13}C$ values of the vegetation in the Linxia Basin are significantly higher (*t*-test, $t=23.76$, d.f.$=245$, $p<0.001$) than the mean $\delta^{13}C$ value of -27.4 ± 1.6‰ ($n=125$) for modern C3 plants [43]. Since the $\delta^{13}C$ of atmospheric CO_2 has decreased by about 1.5‰ due to burning of fossil fuels, it is reasonable to assume a mean value of -25.9 ± 1.6 ($n=125$) for pre-industrial C3 plants, which is still significantly lower than the mean $\delta^{13}C$ value of herbivores' diets in the Linxia Basin (two-tailed *t*-test, $t=13.28$, d.f.$=245$, $p<0.001$). The enriched $\delta^{13}C$ values for herbivores' diets in the Linxia Basin (based on the analysis of fossil enamel) relative to the mean $\delta^{13}C$ value for C3 plants suggest that water-stressed conditions are not a recent phenomenon in the area and probably have existed in the Linxia Basin since the late Oligocene. The carbon isotopic composition of the paleo-atmospheric CO_2 for much of the geologic past cannot be measured directly. Using $\delta^{13}C$ of planktonic foraminifera calcite as a proxy for $\delta^{13}C$ of atmospheric CO_2, Passey et al. [43] reconstructed a time series for $\delta^{13}C$ values associated with C3, water-stressed C3,

Table 1
Stable carbon and oxygen isotopic compositions of fossil enamel apatite from the Linxia Basin

Sample#	Sample name	Locality	$\delta^{3}C$ (PDB)	$\delta^{18}O$ (PDB)	Estimated age (Ma)
Dl-01	Rhinocerotidae	Dalanggou	−8.4	−8.0	17
Dl-02	Rhinocerotidae	Dalanggou	−9.2	−8.1	17
Dl-03	Rhinocerotidae	Dalanggou	−10.7	−8.7	17
Dl-04	*Gomphotherium*	Dalanggou	−9.2	−7.2	17
Dl-05	*Gomphotherium*	Dalanggou	−9.5	−7.3	17
Dl-06	*Gomphotherium*	Dalanggou	−9.0	−6.5	17
Dl-07	*Gomphotherium*	Dalanggou	−8.7	−7.4	17
Dl-08	*Gomphotherium*	Dalanggou	−8.7	−7.4	17
Dl-09	*Gomphotherium*	Dalanggou	−9.3	−6.7	17
Dl-10	*Gomphotherium*	Dalanggou	−9.2	−6.7	17
Ds-01	*Hipparion dermatorhinum*	Dashanzhuang	−10.6	−2.9	6
Ds-02	*Hipparion dermatorhinum*	Dashanzhuang	−10.3	−2.6	6
Ds-03	*Hipparion dermatorhinum*	Dashanzhuang	−10.0	−5.4	6
Ds-04	*Hipparion dermatorhinum*	Dashanzhuang	−9.8	−4.4	6
Ds-05	*Hipparion dermatorhinum*	Dashanzhuang	−10.0	−3.6	6
Ds-06	*Hipparion dermatorhinum*	Dashanzhuang	−10.1	−4.6	6
Ds-07	*Hipparion dermatorhinum*	Dashanzhuang	−9.6	−3.9	6
Ds-08	*Hipparion dermatorhinum*	Dashanzhuang	−9.3	−4.5	6
Ds-09	*Hipparion dermatorhinum*	Dashanzhuang	−10.2	−3.9	6
Ds-10	*Hipparion dermatorhinum*	Dashanzhuang	−9.2	−4.6	6
Ds-11	Rhinocerotidae	Dashanzhuang	−8.9	−4.9	6
Ds-12	Rhinocerotidae	Dashanzhuang	−9.4	−4.9	6
Ds-13	Rhinocerotidae	Dashanzhuang	−9.1	−4.6	6
Ds-14	Rhinocerotidae	Dashanzhuang	−9.8	−7.3	6
Ds-15	Rhinocerotidae	Dashanzhuang	−9.9	−7.1	6
E-11	*Hipparion* sp.	Shanzhuang	−10.0	−8.4	7
E-11	*Hipparion* sp.	Shanzhuang	−10.0	−8.4	7
E-12	Bovidae	Shanzhuang	−8.8	−9.6	7
E-13	*Cervavitus novorassiae*	Shanzhuang	−10.9	−8.1	7
E-14	*Cervavitus novorassiae*	Shanzhuang	−10.9	−7.8	7
E-15	Rhinocerotidae	Shanzhuang	−11.6	−8.8	7
E-16	Rhinocerotidae	Shanzhuang	−11.4	−11.0	7
E-17	Rhinocerotidae	Xinzhuang	−11.4	−8.8	9
E-18	*Samotherium* sp.	Xinzhuang	−10.0	−7.3	9
E-19	*Gazella* sp.	Xinzhuang	−9.7	−7.3	9
E-20	*Cervavitus novorassiae*	Xinzhuang	−9.9	−7.6	9
E-21	*Hipparion* sp.	Xinzhuang	−9.8	−5.8	9
E-22	*Hipparion* sp.	Xinzhuang	−11.5	−9.2	9
E-23	*Samotherium* sp.	Xinzhuang	−9.7	−6.2	9
E-24	*Samotherium* sp.	Xinzhuang	−9.6	−5.4	9
E-25	Rhinocerotidae	Xinzhuang	−11.2	−5.8	9
E-26	*Hipparion* sp.	Xinzhuang	−9.5	−5.2	9
E-27	*Cervavitus novorassiae*	Xinzhuang	−10.0	−6.9	9
E-28	*Gazella* sp.	Xinzhuang	−9.1	−6.6	9
Gn-01	*Hipparion dongxiangense*	Guonigou	−9.1	−3.4	11
Gn-02	*Hipparion dongxiangense*	Guonigou	−8.7	−3.0	11
Gn-03	*Hipparion dongxiangense*	Guonigou	−9.3	−4.3	11
Gn-04	*Hipparion dongxiangense*	Guonigou	−9.4	−2.3	11
Gn-05	*Hipparion dongxiangense*	Guonigou	−10.5	−9.0	11
Gn-06	*Hipparion dongxiangense*	Guonigou	−10.0	−3.0	11

Table 1 (*continued*)

Sample#	Sample name	Locality	$\delta^{3}C$ (PDB)	$\delta^{18}O$ (PDB)	Estimated age (Ma)
Gn-08	*Hipparion dongxiangense*	Guonigou	−9.0	−3.4	11
Gn-11	Rhinocerotidae	Guonigou	−9.8	−4.6	11
Gn-12	Rhinocerotidae	Guonigou	−10.0	−4.6	11
Gn-13	Rhinocerotidae	Guonigou	−9.9	−4.7	11
Gn-14	Rhinocerotidae	Guonigou	−9.8	−4.5	11
Gn-15	Rhinocerotidae	Guonigou	−9.9	−4.5	11
Hl-01	*Hipparion* sp.	Heilinding	−9.7	−5.2	7.5
Hl-02	*Hipparion* sp.	Heilinding	−9.5	−6.3	7.5
Hl-03	*Hipparion* sp.	Heilinding	−9.3	−3.2	7.5
Hl-04	*Hipparion* sp.	Heilinding	−9.4	−5.2	7.5
Hl-05	*Hipparion* sp.	Heilinding	−9.5	−4.0	7.5
Hl-06	*Hipparion* sp.	Heilinding	−9.2	−6.1	7.5
Hl-07	*Hipparion* sp.	Heilinding	−10.2	−6.8	7.5
Hl-10	*Hipparion* sp.	Heilinding	−9.9	−5.1	7.5
Ld-01	*Equus*	Longdan	−10.5	−7.7	2.5
Ld-02	*Equus*	Longdan	−10.6	−8.3	2.5
Ld-03	*Equus*	Longdan	−9.9	−7.9	2.5
Ld-04	*Equus*	Longdan	−11.9	−3.1	2.5
Ld-05	*Equus*	Longdan	−11.9	−3.4	2.5
Ld-06	*Gazella blacki*	Longdan	−11.6	−4.4	2.5
Ld-07	*Gazella blacki*	Longdan	−10.5	−5.6	2.5
Ld-08	*Leptobus amplifrontalis*	Longdan	−10.7	−3.6	2.5
Ld-09	*Leptobus amplifrontalis*	Longdan	−10.5	−5.2	2.5
Ld-10	*Leptobus amplifrontalis*	Longdan	−9.5	−7.1	2.5
Ld-11	*Equus*	Longdan	−8.5	−7.1	2.5
Ld-12	*Equus*	Longdan	−8.8	−8.2	2.5
Ld-12	*Equus*	Longdan	−9.0	−8.1	2.5
Ld-14	*Equus*	Longdan	−9.6	−10.3	2.5
Ld-15	*Equus*	Longdan	−9.3	−9.1	2.5
Ld-17	*Equus*	Longdan	−9.2	−8.1	2.5
Lg-01	Rhinocerotidae	Laogou	−11.7	−8.4	13
Lg-02	Rhinocerotidae	Laogou	−12.4	−9.4	13
Lg-03	Rhinocerotidae	Laogou	−9.8	−8.1	13
Lg-04	Rhinocerotidae	Laogou	−10.8	−10.4	13
Lg-05	Rhinocerotidae	Laogou	−8.9	−8.5	13
Lg-06	*Platybelodon grangeri*	Laogou	−10.1	−8.8	13
Lg-07	*Platybelodon grangeri*	Laogou	−9.6	−8.7	13
Lg-08	*Platybelodon grangeri*	Laogou	−8.9	−7.9	13
Lg-09	*Platybelodon grangeri*	Laogou	−9.2	−7.3	13
Lg-10	*Platybelodon grangeri*	Laogou	−8.8	−7.0	13
Qj-01	*Hipparion dermatorhinum*	Qiaojia	−11.0	−8.4	9.5
Qj-02	*Hipparion dermatorhinum*	Qiaojia	−11.6	−9.5	9.5
Qj-03	*Hipparion dermatorhinum*	Qiaojia	−9.9	−8.6	9.5
Qj-04	*Hipparion dermatorhinum*	Qiaojia	−9.1	−7.2	9.5
Qj-05	*Hipparion dermatorhinum*	Qiaojia	−10.5	−7.2	9.5
Qj-06	*Hipparion dermatorhinum*	Qiaojia	−10.9	−9.9	9.5
Qj-07	Rhinocerotidae	Qiaojia	−12.0	−11.8	9.5
Qj-08	Rhinocerotidae	Qiaojia	−11.4	−9.6	9.5
Qj-09	Rhinocerotidae	Qiaojia	−11.0	−9.6	9.5
Qj-10	Rhinocerotidae	Qiaojia	−11.5	−9.0	9.5
S1-01	*Gazella*	Shilidong	−12.3	−5.9	4
S1-02	*Gazella*	Shilidong	−9.7	−5.6	4
S1-04	*Gazella*	Shilidong	−9.8	−3.8	4

(continued on next page)

Table 1 (*continued*)

Sample#	Sample name	Locality	δ^{3}C (PDB)	δ^{18}O (PDB)	Estimated age (Ma)
S1-05	*Gazella*	Shilidong	−10.5	−5.4	4
S1-06	*Gazella*	Shilidong	−9.6	−8.0	4
S1-07	*Cervavitus novorassiae*	Shilidong	−9.0	−2.8	4
S1-08	*Cervavitus novorassiae*	Shilidong	−10.8	−0.3	4
S1-09	*Palaeotragus microdon*	Shilidong	−10.1	−7.8	4
S1-10	*Palaeotragus microdon*	Shilidong	−10.4	−7.7	4
S1-11	*Hipparion*	Shilidong	−10.3	−4.3	4
S1-12	*Hipparion*	Shilidong	−10.7	−4.3	4
S1-13	*Hipparion*	Shilidong	−10.1	−7.4	4
S1-14	*Hipparion*	Shilidong	−10.2	−6.3	4
S1-15	*Hipparion*	Shilidong	−10.0	−5.7	4
S1-16	*Hipparion*	Shilidong	−10.0	−5.8	4
BY-05	*Equus hemionus*	Beiyuan	−8.2	−5.8	0.05
Tl-01	*Indricotherium*	Tala	−10.3	−12.0	25
Tl-02	*Indricotherium*	Tala	−9.3	−10.7	25
Tl-03	*Indricotherium*	Tala	−10.2	−11.5	25
Tl-04	*Indricotherium*	Tala	−10.4	−11.6	25
Tl-05	*Indricotherium*	Tala	−10.1	−11.4	25
Tl-06	*Allacerops*	Tala	−9.3	−7.1	25
Tl-07	*Allacerops*	Tala	−9.5	−8.2	25
Tl-08	*Allacerops*	Tala	−10.1	−9.5	25
Tl-09	*Allacerops*	Tala	−9.0	−6.8	25
Tz-02	*Equus qingyangensis*	Taizicun	−5.0	−5.6	1

and C4 plant diets over the past 20 Ma. In comparison with the time series enamel δ^{13}C values in Passey et al. [43], many of our fossil enamel δ^{13}C values from the Linxia Basin are greater than the expected values for "average" C3 diets but consistent with water-stressed C3 diets, again suggesting water-stressed conditions have existed in the Linxia Basin throughout much of the late Cenozoic. The δ^{13}C differences among species indicate a mixed habitat in the latest Paleogene and Neogene that probably included riparian wooded habitat or forest (with more negative δ^{13}C values) and more open habitats (with less negative δ^{13}C values) such as woodland/grassland mosaics and C3 grasslands.

Our stable carbon isotope data indicate that C4 plants were either absent or insignificant in the Linxia Basin throughout the latest Paleogene and Neogene. This is in striking contrast to what was observed in Pakistan, Nepal, Africa and the Americas where C4 plants expanded rapidly in the late Miocene, about 7–5 Ma, as indicated by a positive δ^{13}C shift in mammalian tooth enamel and paleosols [4–6,9–15]. Only the paleosol results from the Great Plains [20] and from Tugen Hills, Kenya [19] argue against a late Miocene C4 expansion, among all the records from regions where present ecosystems contain significant amounts of C4 plants. Some of the paleosol carbonates analyzed in the Great Plains study [20] are of questionable origin because the isotopic differences between these carbonates and their co-existing organic matter fall outside the range of 14–17‰ for modern soils (see Fig. 2c in [20]). Similarly, some of the carbonates analyzed in the Tugen Hills study are not clearly of pedogenic origin [19, p. 959]. Therefore it may not be appropriate to interpret the δ^{13}C values of these carbonates in terms of the proportion of C3 vs. C4 plants using the Cerling diffusion model [1,42]. Our carbon isotope data from the Linxia Basin do not show a positive δ^{13}C shift in the late Miocene or early Pliocene. The mean enamel δ^{13}C value prior to 7 Ma is -9.9 ± 0.9‰ and is indistinguishable from the mean δ^{13}C of -10 ± 0.9‰ for the period of 7 to 2.5 Ma (see Table 3).

Table 2
Stable carbon isotopic composition of pedogenic carbonate and soil organic matter in the Linxia Basin

Sample#	$\delta^{13}C$ (PDB)	Estimated %C4	Sample type	Estimated age
YJS-0-1	−6.1	39	Soil carbonate nodule	Modern
YJS-0-2	−6.3	38	Soil carbonate nodule	Modern
YJS-1-1	−7.5	30	Soil carbonate nodule	Modern
YJS-1-2	−6.4	37	Soil carbonate nodule	Modern
YJS-1-3	−6.5	36	Soil carbonate nodule	Modern
YJS-17-1	−6.0	40	Soil carbonate nodule	Modern
YJS-17-2	−5.4	44	Soil carbonate nodule	Modern
YJS-20-1	−7.7	29	Soil carbonate nodule	Modern
YJS-20-2	−8.5	24	Soil carbonate nodule	Modern
YJS-23-1	−7.0	34	Soil carbonate nodule	Modern
YJS-23-2	−6.3	38	Soil carbonate nodule	Modern
YJS-26	−8.6	23	Soil carbonate nodule	Modern
YJS-8-1	−6.9	34	Soil carbonate nodule	Modern
YJS-8-2	−7.9	27	Soil carbonate nodule	Modern
YJS-19-1	−8.4	24	Soil carbonate nodule	L. Pleistocene
YJS-19-2	−8.0	27	Soil carbonate nodule	L. Pleistocene
YJS-2-1	−6.7	35	Soil carbonate nodule	L. Pleistocene
YJS-2-2	−7.4	31	Soil carbonate nodule	L. Pleistocene
YJS-25-1	−7.8	28	Soil carbonate nodule	L. Pleistocene
YJS-25-2	−7.0	34	Soil carbonate nodule	L. Pleistocene
YJS-2-3a	−8.0	27	Carbonate nodule w/growth layers, outer layer	L. Pleistocene
YJS-2-3b	−7.1	33	Carbonate nodule w/growth, inner darker layer	L. Pleistocene
YJS-2-4a	−7.4	31	Carbonate nodule w/growth layers, outer layer	L. Pleistocene
YJS-2-4b	−6.7	35	Carbonate nodule w/growth, inner darker layer	L. Pleistocene
BY-2-1	−6.8	35	Carbonate coating on pebble	M. Pleistocene
BY-2-2	−6.3	38	Pedogenic carbonate coating on pebble	M. Pleistocene
YJS-16	−22.6	32	Soil organic matter	Modern
YJS-18	−25.2	13	Soil organic matter	Modern
YJS-21	−23.6	25	Soil organic matter	Modern
YJS-22	−22.8	30	Soil organic matter	L. Pleistocene
YJS-24	−23.5	25	Soil organic matter	L. Pleistocene

(2) ~2.5 Ma to present: In contrast to the previous period, horse tooth enamel samples (*Equus hemionus* and *Equus qingyangensis*) collected from the Lishi Loess (middle Pleistocene) and Malan Loess (late Pleistocene) have a mean $\delta^{13}C$ value of $-6.6 \pm 2.3‰$ (Fig. 3a), which is significantly higher ($p < 0.001$) than the mean $\delta^{13}C$ value for the previous period (Table 3) and indicates a dietary intake of ~40% C4 plants. The presence of significant amounts of C4 grasses in the horses' diet indicates that C4 grasses had become a part of the local ecosystems in the Pleistocene. The existence of C4 plants in the area during the Quaternary is also supported by the $\delta^{13}C$ data from Pleistocene paleosols as discussed below.

The present-day climate in the Linxia Basin is strongly influenced by East Asian monsoon system originated from the contrast in heat capacity between the land and the sea [44]. The mean annual temperature in the basin is 7 °C, the growing season (May–September) temperatures range between 11 and 30 °C (or 52 and 86 °F), and annual rainfall is about 515 mm with most of the rain falling in the summer. The minimum July temperature is 18 °C (or 64 °F). Teeri and Stowe [8] found a very strong correlation between the minimum July temperature and the species abundance of C4 grasses in the flora of North America. If this correlation holds for China, the present-day minimum July temperature in the Linxia Basin would predict a

Table 3
Two-tailed *t*-test results for significant isotopic differences between mean isotopic values of different ages

	Mean difference (‰)	*df*	*t*	*p*	Significant difference at 95%?
$\delta^{13}C$ (>7Ma) vs. $\delta^{13}C$ (7–2.5Ma)	0.2	122	1.24	0.22	No
$\delta^{13}C$ (2.5Ma and older) vs. $\delta^{13}C$ (post 2.5Ma)	3.4	124	5.27	<0.0001	Yes
Horse-$\delta^{18}O$ (11Ma) vs. horse-$\delta^{18}O$ (9.5Ma)	4.4	11	4.27	0.001	Yes
Horse-$\delta^{18}O$ (9.5Ma) vs. horse-$\delta^{18}O$ (9Ma)	1.7	7	1.63	0.15	No
Horse-$\delta^{18}O$ (9Ma) vs. horse-$\delta^{18}O$ (7.5Ma)	1.5	9	1.54	0.16	No
Horse-$\delta^{18}O$ (9.5Ma) vs. horse-$\delta^{18}O$ (7.5Ma)	3.2	12	5.13	0.0002	Yes
Horse-$\delta^{18}O$ (7.5Ma) vs. horse-$\delta^{18}O$ (7Ma)	3.2	8	3.66	0.006	Yes
Horse-$\delta^{18}O$ (7Ma) vs. horse-$\delta^{18}O$ (6Ma)	4.4	10	7.13	<0.0001	Yes
Horse-$\delta^{18}O$ (6Ma) vs. horse-$\delta^{18}O$ (2.5Ma)	3.4	19	4.4	0.00025	Yes
Horse-$\delta^{18}O$ (2.5Ma) vs. horse-$\delta^{18}O$ (<2.5Ma)	1.7	10	2.55	0.028	Yes
Rhino-$\delta^{18}O$ (11Ma) vs. rhino-$\delta^{18}O$ (9.5Ma)	5.4	7	9.83	<0.0001	Yes
Rhino-$\delta^{18}O$ (9.5Ma) vs. rhino-$\delta^{18}O$ (9Ma)	2.7	4	2.04	0.11	No
Rhino-$\delta^{18}O$ (7Ma) vs. rhino-$\delta^{18}O$ (6Ma)	4.1	5	3.56	0.016	Yes
Deer-$\delta^{18}O$ (7Ma) vs. deer-$\delta^{18}O$ (4Ma)	6.4	2	5.01	0.038	Yes
Bovid-$\delta^{18}O$ (7Ma) vs. bovid-$\delta^{18}O$ (4Ma)	3.9	5	3.44	0.018	Yes

Bold highlights the 7 Ma shift.

C4 species abundance of ~40% or less. The $\delta^{13}C$ values of pedogenic carbonates from modern soils range from −5.4‰ to −8.6‰ (Table 2), with a mean $\delta^{13}C$ value of -6.9 ± 1.0‰. These values indicate mixed C3 and C4 vegetation that is unevenly distributed over the landscape with C4 plants making up about 13% to 43% of the biomass in the basin in the Holocene. Pedogenic carbonates from buried paleosols formed in Pleistocene loess deposits have $\delta^{13}C$ values varying from −6.3‰ to −8.4‰, which indicate a mixed C3 and C4 vegetation with approximately 24–35% C4 grasses in the Pleistocene (Table 2). The carbon isotopic differences between paleosol carbonates and coexisting organic matter are 15–16‰ and are well within the expected range for modern soils [1], suggesting that the isotopic compositions of these soil components had not been diagenetically altered. Both our soil and tooth enamel isotopic data from the Linxia Basin indicate that C4 grasses have been an important component of local ecosystems in the Quaternary.

4.2. Oxygen isotopes and climate change

$\delta^{18}O$ of tooth enamel is related to the $\delta^{18}O$ of local meteoric water, which provides drinking water for most animals and water for plants that are consumed by herbivores. Because the $\delta^{18}O$ of meteoric water is controlled by climatic conditions [45,46], a shift in $\delta^{18}O$ of tooth enamel of the same species indicates a change in some aspects of regional climate [e.g.,2,3,9,47–51].

In northern Pakistan and Nepal, the change from C3 to C4 vegetation occurred around 7–8 Ma and was accompanied by a shift in $\delta^{18}O$ values of soil carbonate and tooth enamel [9,13]. In the Linxia Basin, there was no carbon isotopic shift in mammalian tooth enamel in the late Miocene. However, the $\delta^{18}O$ values of tooth enamel from horses and rhinos (which cover a longer time period than other groups analyzed) show several significant shifts during the late Cenozoic (Fig. 4, Table 3). The large range of $\delta^{18}O$ values within the horse and rhino families at a given time interval (Figs. 3 and 4) may reflect differences in the drinking and dietary behaviors of different species and seasonal variability of $\delta^{18}O$ of local rainfall [3,52]. Therefore, the mean $\delta^{18}O$ values are more meaningful than individual data for understanding regional climatic trends because they attenuate $\delta^{18}O$ variability caused by behavioral, local and seasonal processes [3].

As shown in Fig. 4a and Table 3, the $\delta^{18}O$ of tooth enamel from horses shifted significantly ($p<0.01$) to more negative values after ~11, ~7.5, and ~6 Ma. These negative oxygen isotopic shifts indicate changes in climate towards cooler temperatures and/or less arid

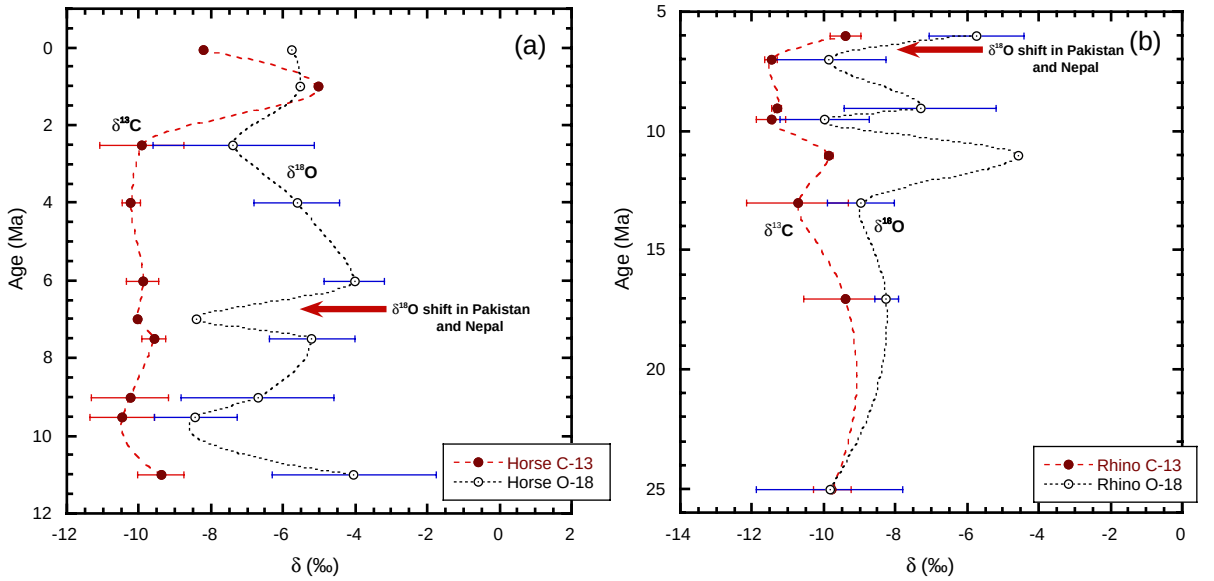

Fig. 4. The average δ^{13}C and δ^{18}O values of tooth enamel of horses (a) and rhinos (b) from the Linxia Basin in northern China. The bars indicate the standard deviation.

conditions. Similarly, there are significant δ^{18}O shifts towards higher values after ~9.5, ~7, and ~2.5 Ma (Table 3, Fig. 4a), which indicate shifts to warmer and/or drier conditions. The enamel δ^{18}O values from rhinos also show parallel shifts where there is data coverage (Fig. 4b, Table 3). Most notably, the positive δ^{18}O shift after ~7 Ma, which is also seen in deer and bovid (Table 3 and Fig. 3b), is comparable in timing and direction to the δ^{18}O shift observed in paleosol carbonates and fossil enamel in Pakistan and Nepal [9,12,13], indicating a change in climatic conditions on both sides of the plateau at about the same time in the late Miocene. Diagenesis does not seem to have modified the isotopic composition of the enamel because this 7-Ma δ^{18}O shift occurred in all the species (i.e., horse, rhino, deer and bovid) found for this particular time interval (Table 3, Fig. 3b). The significant isotopic difference between the tooth enamel and matrix also argues against significant diagenetic alteration of the isotopic signatures of the tooth enamel (Fig. 5). Recent oxygen isotope analysis of fluvial and lacustrine carbonates from the Linxia Basin suggests a shift to more arid conditions at 12 Ma [53]. Although the time resolution of our Miocene samples does not permit direct comparison of our data with the oxygen isotope data in Dettman et al. [53], our data also show a large positive shift from ~13 to 11 Ma (Fig. 4b, Table 3), suggesting a shift towards more arid conditions and/or higher temperatures.

The deep-sea δ^{18}O and Mg/Ca records reveal a general cooling trend for the past 50 Ma with two main cooling phases over the past 25 Ma [54–58]. These cooling phases are associated with major ice sheet expansions in the late Middle Miocene and in the Plio–Pleistocene [54,57,59]. Our tooth-enamel δ^{18}O data do not cover the late Middle Miocene climatic events in any detail. But the tooth-enamel δ^{18}O data from the Linxia Basin show a general shift to more negative values from about ~6 to ~2.5 Ma (Fig. 4a), indicating a shift to cooler temperatures. This is in broad agreement with the marine δ^{18}O and Mg/Ca records [57,58].

4.3. The timing of C4 expansion in northern China and the rise of the Tibetan Plateau

Although C4 plants did not spread into the Linxia Basin during the period of "global C4 expansion" (i.e., ~7–5 Ma) until the Quaternary, previously published paleosol carbonate isotopic data from the Loess Plateau [60] and tooth enamel isotopic data from several other localities [61,62] in northern China in-

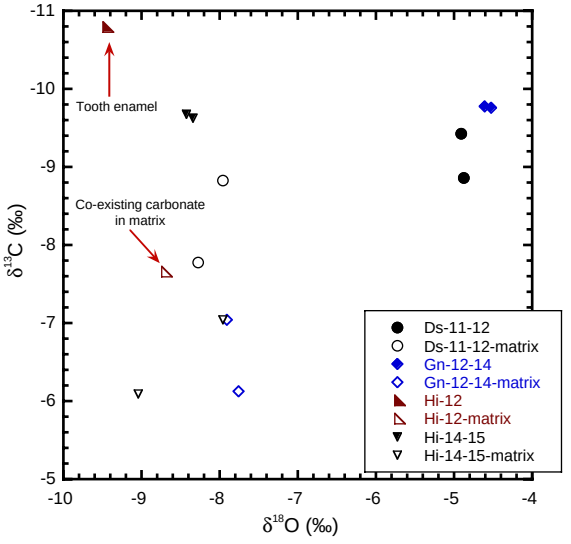

Fig. 5. Carbon and oxygen isotopic compositions of tooth enamel and coexisting carbonate in matrix. Different symbols represent samples from different stratigraphic units. Filled symbol represents tooth enamel and the corresponding open symbol represents the coexisting carbonate in matrix (arrows indicate one such pair of enamel and co-existing carbonate in matrix as an example). This shows that the $\delta^{13}C$ and $\delta^{18}O$ values of tooth enamel are very different from those of co-existing carbonate in the matrix, indicating little or no diagenetic alteration of the isotopic composition of tooth enamel.

dicate that C4 grasses had become a significant component of local ecosystems in northern China by the Plio–Pleistocene (Fig. 6). In a recent isotopic study of paleosol carbonates in a late Cenozoic red-clay and loess sequence at Lingtai on the Loess Plateau, Ding and Yang [63] suggested that C4 plants expanded at ~4 Ma on the Loess Plateau, but not driven by climate change because their data show no changes in the $\delta^{18}O$ of paleosol carbonates for the past 7 million years. Our oxygen isotope data from the Linxia Basin on the other hand reveal significant shifts in climate during the late Cenozoic. Although the available data from China seem to suggest that the "late Miocene C4 expansion" did not occur in northern China, these data are not sufficient to provide conclusive proof that the expansion of C4 grasses in northern China occurred much later than in the similar latitudes in other parts of the world. The earliest definitive C4 signal in fossil enamel from China is from Yushe (Fig. 6) which is located further east of the Linxia Basin (Fig. 1), but unfortunately there are no older samples currently available from Yushe to determine the timing of C4 expansion at the site. Was there an east–west gradient in the expansion of C4 grasses in northern China associated with temperature and precipitation gradient caused by the uplift of the Tibetan plateau [64]? Comparable late Neogene paleovegetation and paleoclimate records from localities outside the Linxia Basin are needed to answer this question, to test the hypotheses concerning the late Miocene "global expansion" of C4 plants, and to help understand the interplay between the development of C4 ecosystems and natural climate variability.

In the present-day semi-arid grasslands in the Linxia Basin, C4 grasses make up a significant component of the biomass, as indicated by our carbon isotope data from modern soils (Table 2) and a plant survey by Yin and Li [65]. The lack of C4 plants in the Linxia Basin prior to ~2–3 Ma indicates that the climatic conditions in the area were not favorable for C4 plants until then. The present-day climate in northern China is strongly influenced by Asian monsoons, which dominate the seasonal wind and precipitation patterns and the character of land vegetation [66]. In the summer, the East Asian summer monsoon and the Indian monsoon carry warm wet air from the Pacific

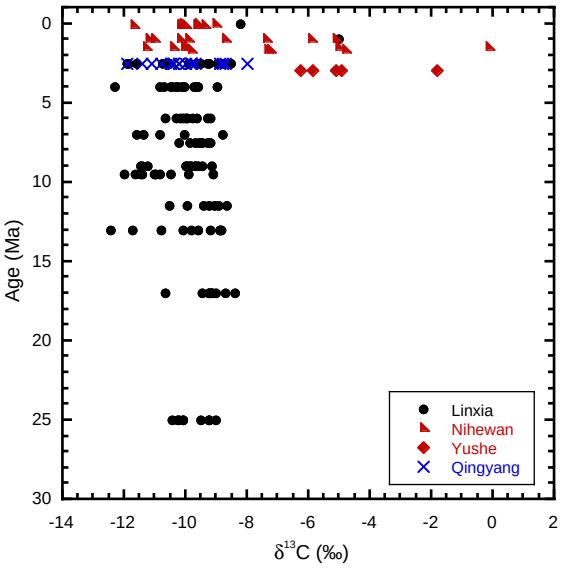

Fig. 6. Stable carbon isotopic ratios of herbivore tooth enamel from several localities (shown in Fig. 1) in northern China: Linxia (this study), Qingyang [62], Nihewan [61] and Yushe (our unpublished data).

and Indian oceans to the interior, resulting in an increase in precipitation and the creation of favorable conditions for the growth of C4 grasses. In the winter, the East Asian winter monsoon brings cold and dry air from Siberia southward across China. The advance and retreat of the summer/winter monsoons result in the strong seasonality of precipitation and temperature. The lack of C4 plants in the Linxia Basin prior to ~2–3 Ma suggests that the East Asian summer monsoon system, currently controlling the climatic conditions in the basin, was not strong enough to affect this part of northern China during much of the Neogene, which implies that the elevation of most of the Himalayan-Tibetan plateau was below a threshold for the development or strengthening of the East Asian summer monsoon. This suggests that significant uplift occurred more recently, supporting the view that a major surface uplift event occurred during the Pliocene and Quaternary [e.g., 67–69]. Alternatively, the late C4 expansion in the Linxia Basin could be caused by an early attainment of a high altitude where cooler temperatures delayed the expansion of C4 grasses until the atmospheric pCO_2 declined further, which would support the view that the current elevation/extent of the Himalayan-Tibetan plateau was reached by late Miocene [e.g.,70,71] and the hypothesis that the C4 expansion was driven by declining atmospheric CO_2 [6]. However, proxy records of paleo-atmospheric pCO_2 suggest that the atmospheric pCO_2 has remained low without major changes since the early Miocene [21–23]. Therefore, the most plausible explanation is as follows. Although significant surface uplift of the Himalayan-Tibetan plateau may have occurred much earlier, the elevation/extent of much of the high plateau was probably below a threshold to support a strong East Asian monsoon system until after ~2.5 Ma. More recent uplift in the Plio–Pleistocene further strengthened the land-sea thermal contrast and intensified the Asian summer monsoons, creating favorable conditions for expansion of C4 grasses into the area. This implies that much of the current elevation/extent of the plateau was probably reached after ~2–3 Ma.

In the Linxia Basin, C4 expansion did not occur in the late Miocene. However, the oxygen isotopic ratios of tooth enamel shifted dramatically towards higher values from ~7 to 6 Ma (Fig. 4). This late Miocene $\delta^{18}O$ shift indicates a change in climate and is comparable in timing and direction to the $\delta^{18}O$ shift observed in Pakistan and Nepal. The $\delta^{18}O$ shift in Pakistan and Nepal was interpreted as indicative of rapid uplift of the Himalayan-Tibetan Plateau in the late Miocene, which strengthened the land–sea thermal contrast, intensified monsoonal circulation and caused the C4 grass expansion [12–14,64,72]. However, our carbon isotope data do not support a strong summer monsoon in the Linxia Basin prior to ~2–3 Ma. This late Miocene climate change seems to be a global phenomenon as inferred from a variety of data from many parts of the world including areas outside the direct influence of the Asian monsoons e.g., [9,12,13,15,73–78]. The 7-Ma $\delta^{18}O$ shift in tooth enamel and paleosols observed on both sides of the Himalaya and the Tibetan Plateau is therefore most likely a regional manifestation of a global climate change.

5. Conclusions

Carbon and oxygen isotopic analyses of mammalian tooth enamel and soils reveal significant changes in vegetation and climate over the past 25 Ma in the Linxia Basin at the northeastern margin of the Tibetan Plateau. The pure or nearly pure C3 diet for various herbivores prior to ~2–3 Ma suggests that the landscape in the area was dominated by C3 plants, most likely in a mixed habitat including woodland/grassland mosaics, C3 grasslands and forests. On the other hand, carbon isotope data from tooth enamel and soils of Pleistocene and Holocene ages indicate that C4 grasses have been an important component of local ecosystems in the Quaternary. The $\delta^{18}O$ values of tooth enamel from the Linxia Basin record several significant shifts in regional climate during the Neogene. Although the collision of the Indian Plate onto the Eurasian Plate had caused significant surface uplift of the Himalayan-Tibetan plateau before the end of the Miocene, the lack of C4 grasses in the Linxia Basin prior to ~2–3 Ma suggests that the elevation of most of the high plateau was probably below a threshold such that the East Asian summer monsoon had little influence in this part of China until after ~2.5 Ma. More recent uplift in the Plio–Pleistocene further strengthened the land–sea thermal contrast and intensified the Asian summer monsoons, creating favorable

conditions for expansion of C4 grasses into the area. We suggest that the strengthening of the East Asian summer monsoon due to the rapid uplift of the Himalayan-Tibetan plateau likely triggered the expansion of C4 grasses into this part of China.

Acknowledgements

This research was funded by U.S. National Science Foundation (INT-0204923 to Wang), Chinese National Science Foundation (NSFC 40232023 to Deng) and Chinese Academy of Sciences (KZCX2-103 and RJZ2001-105 to Deng). We thank Yonghoon Choi, Dr. Jason Curtis, Mabry Gaboardi and Dana Biasatti for assistance in sample preparation and analyses; Drs. David Fox and Lawrence Flynn and an anonymous reviewer for helpful reviews of this paper.

References

[1] T.E. Cerling, J. Quade, Y. Wang, J. Bowman, Carbon isotopes in soils and palaeosols as ecology and palaeoecology indicators, Nature 341 (1989) 138–139.
[2] P. Koch, Isotopic reconstruction of past continental environments, Annu. Rev. Earth Planet. Sci. 26 (1998) 573–613.
[3] M. Kohn, T.E. Cerling, Stable isotope compositions of biological apatite, in: M. Kohn, J. Rakovan, J. Hughes (Eds.), Phosphates—Geochemical, Geobiological, and Materials Importance, Reviews in Mineralogy and Geochemistry, vol. 48, Mineralogical Society of America, Washington D.C., 2002, pp. 455–488.
[4] T.E. Cerling, Y. Wang, J. Quade, Expansion of C4 ecosystems as an indicator of global ecological change in the late Miocene, Nature 361 (1993) 344–345.
[5] T.E. Cerling, J. Harris, B. MacFadden, Carbon isotopes, diets of North American equids, and the evolution of North American C4 grasslands, in: H. Griffiths, D. Robinson, P. van Gardingen (Eds.), Stable isotopes and the integration of biological, ecological, and geochemical processes, Bios Scientific Publishers, Oxford, 1997, pp. 363–379.
[6] T.E. Cerling, J. Harris, B. MacFadden, M. Leakey, J. Quade, V. Eisenmann, J. Ehleringer, Global vegetation change through the Miocene–Pliocene boundary, Nature 389 (1997) 153–158.
[7] L. Tieszen, M. Senyimba, S. Imbamba, J. Troughton, The distribution of C3 and C4 grasses and carbon isotopic discrimination along an altitudinal and moisture gradient in Kenya, Oecologia 37 (1979) 337–350.
[8] J. Teeri, L. Stowe, Climatic patterns and the distribution of C4 grasses in North America, Oecologia 23 (1976) 1–12.
[9] J. Quade, T.E. Cerling, J. Barry, M. Morgan, D. Pilbeam, A. Chivas, J. Lee-Thorp, N. van der Merwe, A 16-Ma record of paleodiet using carbon and oxygen isotopes in fossil teeth from Pakistan, Chem. Geol. 94 (1992) 183–192.
[10] Y. Wang, T.E. Cerling, B. MacFadden, Fossil horses and carbon isotopes: new evidence for Cenozoic dietary, habitat, and ecosystem changes in North America, Palaeogeogr. Palaeoclimatol. Palaeoecol. 107 (1994) 269–279.
[11] B. MacFadden, T. Cerling, J. Prado, Cenozoic terrestrial ecosystem evolution in Argentina: evidence from carbon isotopes of fossil mammal teeth, PALAIOS 11 (1996) 319–327.
[12] J. Quade, T.E. Cerling, J.R. Bowman, Development of Asian monsoon revealed by marked ecological shift during latest Miocene in northern Pakistan, Nature 342 (1989) 163–166.
[13] J. Quade, J. Carter, T. Ojha, J. Adams, T. Harrison, Late Miocene environmental change in Nepal and the northern Indian subcontinent: stable isotopic evidence from paleosols, Geol. Soc. Amer. Bull. 107 (1995) 1381–1397.
[14] J. Quade, T.E. Cerling, Expansion of C4 grasses in the late Miocene of Northern Pakistan: evidence from stable isotopes in paleosols, Palaeogeogr. Palaeoclimatol. Palaeoecol. 115 (1995) 91–116.
[15] C. Latorre, J. Quade, W. McIntosh, The expansion of C4 grasses and global change in the late Miocene: stable isotope evidence from the Americas, Earth Planet. Sci. Lett. 146 (1997) 83–96.
[16] B. MacFadden, Y. Wang, T.E. Cerling, F. Anaya, South American fossil mammals and carbon isotopes: a 25 million-year sequence from the Bolivian Andes, Palaeogeogr. Palaeoclimatol. Palaeoecol. 107 (1994) 257–268.
[17] B. MacFadden, T. Cerling, Fossil horses, carbon isotopes and global change, Trends Ecol. Evol. 9 (1994) 481–485.
[18] M. Morgan, J. Kingston, B. Marino, Carbon isotopic evidence for the emergence of C4 plants in the Neogene from Pakistan and Kenya, Nature 367 (1994) 162–164.
[19] J. Kingston, B. Marino, A. Hill, Isotopic evidence for Neogene hominid paleoenvironments in the Kenya Rift Valley, Science 264 (1994) 955–958.
[20] D. Fox, P. Koch, Tertiary history of C4 biomass in the Great Plains, USA, Geology 31 (2003) 809–812.
[21] A. Hill, in: E. Vrba, G. Denton, T. Partridge, L. Burckle (Eds.), Paleoclimate and Evolution with Emphasis on Human Origins, Yale Univ Press, New Haven, 1995, pp. 178–193.
[22] M. Pagani, K. Freeman, M. Arthur, Late Miocene atmospheric CO_2 concentrations and the expansion of C4 grasses, Science 285 (1999) 876–879.
[23] P. Pearson, M. Palmer, Atmospheric carbon dioxide concentrations over the past 60 million years, Nature 406 (2000) 695–699.
[24] Y. Fan, X. Du, The National Physical Atlas of China, China Cartographic Publishing House, Beijing, China, 1998, 230 pp.
[25] G. Ren, H. Beug, Mapping Holocene pollen data and vegetation of China, Quat. Sci. Rev. 21 (2002) 1395–1422.
[26] Z. Qiu, W. Wu, Z. Qiu, Miocene mammal fauna sequence of China: palaeozoogeography and Eurasian relationships, in: G. Rossner, K. Heissig (Eds.), The Miocene Land Mammals of Europe, Verlag Dr Friedrich Pfeil, Munchen, 1999, pp. 443–455.

[27] X.M. Fang, J.J. Li, J.J. Zhu, H. Chen, J.X. Cao, Determination and calibration of time scale of late Cenozoic sedimentary sequences in Linxia basin, Gansu Province, Chin. Sci. Bull. 42 (1997) 1457–1471.
[28] X.M. Fang, C. Garzione, R. Van der Voo, J. Li, J. Fan, Flexural subsidence by 29 Ma on the NE edge of Tibet from the magnetostratigraphy of Linxia Basin, China, Earth Planet. Sci. Lett. 210 (2003) 545–560.
[29] T. Deng, X.M. Wang, X.J. Ni, L.P. Liu, Z. Liang, Cenozoic stratigraphic sequence of the Linxia Basin in Gansu, China and its evidence from mammal fossils, Vertebrata Palasiatica 42 (2004) 45–66.
[30] A. Yin, T.M. Harrison, Geologic evolution of the Himalayan-Tibetan orogen, Annu. Rev. Earth Planet. Sci. 28 (2000) 211–280.
[31] P. Tapponnier, Z. Xu, F. Roger, B. Meyer, N. Arnaud, G. Wittlinger, J. Yang, Oblique stepwise rise and growth of the Tibet Plateau, Science 294 (2001) 1671–1677.
[32] J. Lee-Thorp, N. van der Merwe, Carbon isotope analysis of fossil bone apatite, S. Afr. J. Sci. 83 (1987) 712–715.
[33] Y. Wang, T.E. Cerling, B. Effland, Stable isotope ratios of soil carbonate and soil organic matter as indicators of forest invasion of prairie near Ames, Iowa, Oecologia 95 (1993) 365–369.
[34] J. Lee-Thorp, N. van der Merwe, C. Brian, Isotopic evidence for dietary differences between two extinct baboon species from Swartkrans, J. Hum. Evol. 18 (1989) 183–190.
[35] T.E. Cerling, J.M. Harris, Carbon isotope fractionation between diet and bioapatite in ungulate mammals and implications for ecological and paleoecological studies, Oecologia 120 (1999) 347–363.
[36] P. Deines, The isotopic composition of reduced organic carbon, in: P. Fritz, J. Fontes (Eds.), The Terrestrial Environment, Handbook of Environmental Isotope Geochemistry, vol. 1, Elsevier, Amsterdam, 1980, pp. 329–406.
[37] M. O'Leary, Carbon isotopes in photosynthesis, Bioscience 38 (1988) 328–335.
[38] G. Farquhar, J. Ehleringer, K. Hubick, Carbon isotope discrimination and photosynthesis, Annu. Rev. Plant Physiol. Plant Mol. Biol. 40 (1989) 503–537.
[39] G. Schleser, R. Jayasekera, $\delta^{13}C$ variations of leaves in forests as an indication of reassimilated CO_2 from the soil, Oecologia 65 (1985) 536–542.
[40] L. Sternberg, S. Mulkey, S. Wright, Ecological interpretation of leaf carbon isotope ratios: influence of respired carbon dioxide, Ecology 70 (1989) 1317–1324.
[41] N. Van der Merwe, E. Medin, Photosynthesis and $^{13}C/^{12}C$ ratios in Amazon rain forests, Geochim. Cosmochim. Acta 53 (1989) 1091–1094.
[42] T.E. Cerling, The stable isotopic composition of modern soil carbonate and its relationship to climate, Earth Planet. Sci. Lett. 71 (1984) 229–240.
[43] B. Passey, T. Cerling, M. Perkins, M. Voorhies, J. Harris, S. Tucker, Environmental change in the great plains: an isotopic record from fossil horses, J. Geol. 110 (2002) 123–140.
[44] Z. An, J. Kutzbach, W. Prell, S. Porter, Evolution of Asian monsoons and phased uplift of the Himalayan-Tibetan plateau since late Miocene times, Nature 411 (2001) 62–66.
[45] W. Dansgaard, Stable isotopes in precipitation, Tellus 16 (1964) 436–468.
[46] K. Rozanski, L. Araguas-Araguas, R. Gonfiantini, Relation between long-term trends of oxygen-18 isotope composition of precipitation and climate, Science 258 (1992) 981–985.
[47] J.D. Bryant, B. Luz, P. Froelich, Oxygen isotopic composition of fossil horse tooth phosphate as a record of continental paleoclimate, Palaeogeogr. Palaeoclimatol. Palaeoecol. 107 (1994) 303–316.
[48] H. Fricke, J. O'Neil, N. Lynnerup, Oxygen isotope composition of human tooth enamel from medieval Greenland: linking climate and society, Geology 23 (1995) 869–872.
[49] L. Ayliffe, A. Chivas, Oxygen isotope composition of the bone phosphate of Australian kangaroos: potential as a palaeoenvironmental recorder, Geochim. Cosmochim. Acta 54 (1990) 2603–2609.
[50] L. Ayliffe, A. Lister, A. Chivas, The preservation of glacial–interglacial climatic signatures in the oxygen isotopes of elephant skeletal phosphate, Palaeogeogr. Palaeoclimatol. Palaeoecol. 99 (1992) 179–191.
[51] L. Ayliffe, A. Chivas, M. Leakey, The retention of primary oxygen isotope compositions of fossil elephant skeletal phosphate, Geochim. Cosmochim. Acta 58 (1994) 5291–5298.
[52] B. MacFadden, Tale of two rhinos: isotopic ecology, paleodiet, and niche differentiation of *Aphelops* and *Teleoceras* from the Florida Neogene, Paleobiology 24 (1998) 274–286.
[53] D. Dettman, X. Fang, C. Garzione, J. Li, Uplift-driven climate change at 12 Ma: a long $\delta^{18}O$ record from the NE margin of the Tibetan Plateau, Earth Planet. Sci. Lett. 214 (2003) 267–277.
[54] N. Shackleton, J. Kennett, Paleotemperature history of the Cenozoic and the initiation of Antarctic glaciation: oxygen and carbon isotope analyses in DSDP sites 277, 279, and 281, Initial Rep. Deep Sea Drill. Proj. Leg. 29 (1975) 743–955.
[55] N. Shackleton, M. Hall, D. Pate, Pliocene stable isotope stratigraphy of site 846, Proc. ODP Sci. Res. 138 (1995) 337–355.
[56] K. Miller, R. Fairbanks, G. Mountain, Tertiary oxygen isotope synthesis, sea level history, and continental margin erosion, Paleoceanography 2 (1987) 1–19.
[57] C. Lear, H. Elderfield, P. Wilson, Cenozoic deep-sea temperatures and global ice volumes from Mg/Ca in benthic foraminiferal calcite, Science 287 (2000) 269–272.
[58] J. Zachos, M. Pagani, L. Sloan, E. Thomas, K. Billups, Trends, rhythms, and aberrations in global climate 65 Ma to present, Science 292 (2001) 686–693.
[59] B. Flower, J. Kennett, Middle Miocene deepwater paleoceanography in the southwest Pacific: relations with East Antartic Ice Sheet Development, Paleoceanography 10 (1995) 1095–1112.
[60] Y. Wang, S.H. Zheng, Paleosol nodules as Pleistocene paleoclimatic indicators, Luochuan, P. R. China, Palaeogeogr. Palaeoclimatol. Palaeoecol. 76 (1989) 39–44.

[61] T. Deng, J. Dong, Y. Wang, Variation of terrestrial ecosystem recorded by stable carbon isotopes of fossils in northern China during the Quatenary, Chin. Sci. Bull. 47 (2002) 76–77.
[62] T. Deng, X. Xue, J. Dong, The evidence of fossil carbon isotopes of the climatic event at the beginning of Quaternary, Chin. Sci. Bull. 44 (1999) 477–480.
[63] Z. Ding, S. Yang, C3/C4 vegetation evolution over the last 7.0 Myr in the Chinese Loess Plateau: evidence from pedogenic carbonate $\delta^{13}C$, Palaeogeogr. Palaeoclimatol. Palaeoecol. 160 (2000) 291–299.
[64] J. Kutzbach, W. Prell, W. Ruddiman, Sensitivity of Eurasian climate to surface uplift of the Tibetan Plateau, J. Geol. 101 (1993) 177–190.
[65] L. Yin, M. Li, A study of the geographic distribution and ecology of C4 plants in China: I. C4 plant distribution in China and their relation with regional climatic condition, Acta Ecol. Sin. 17 (1997) 350–363.
[66] X. Liu, A. Yin, Sensitivity of East Asia monsoon climate to the uplift of the Tibetan Plateau, Palaeogeogr. Palaeoclimatol. Palaeoecol. 183 (2002) 223–245.
[67] X. Ren, Geological and Ecological Studies of Qinghai–Xizang (Tibet) Plateau, vol. 1, 1981, pp. 139–143.
[68] W. Chen, Pliocene environment of *Hipparion* Fauna of Middle Himalaya Range, Vertebrata Palasiatica 20 (1982) 45–54.
[69] H. Zheng, C. Powell, Z. An, J. Zhou, G. Dong, Pliocene uplift of the northern Tibetan Plateau, Geology 28 (2000) 715–718.
[70] T.M. Harrison, P. Copeland, W.S.F. Kidd, An Yin, Raising Tibet, Science 255 (1992) 1663–1670.
[71] P. Molnar, P. England, J. Martinod, Mantle dynamics, uplift of the Tibetan Plateau, and the Indian monsoon, Rev. Geophys. 31 (1993) 357–396.
[72] W. Prell, J. Kutzbach, Sensitivity of the Indian monsoon to forcing parameters and implications for its evolution, Nature 360 (1992) 647–652.
[73] L. Burkle, Distribution of diatoms in the northern Indian Ocean: relationship to physical oceanography, Mar. Micropaleontol. 15 (1989) 53–65.
[74] D. Rea, H. Snoeckx, L. Joseph, Late Cenozoic eolian deposition in the North Pacific: Asian drying, Tibetan uplift, and cooling of the northern hemisphere, Paleoceanography 13 (1998) 215–224.
[75] J. Barry, L. Flynn, Key biostratigraphic events in the Siwalik sequence, in: E.H. Lindsay, et al., (Eds.), European Neogene Mammal Chronology, Plenum Press, New York, 1990, pp. 557–571.
[76] L. Flynn, L. Jacobs, Effects of changing environments on Siwalik rodent faunas of northern Pakistan, Palaeogeogr. Palaeoclimatol. Palaeoecol. 38 (1982) 129–138.
[77] D. Kroon, T. Steens, S. Troelstra, Onset of monsoonal related upwelling in the western Arabian Sea as revealed by planktonic foraminifers, ODP, Sci. Res. 117 (1991) 257–263.
[78] T.E. Cerling, Development of grasslands and savannas in East Africa during the Neogene, Palaeogeogr. Palaeoclimatol. Palaeoecol. 97 (1992) 241–247.